CHINESE OPTICS LETTERS

Vol. 20, No. 10 | October 2022

Sub-30 fs Yb-fiber laser source based on a hybrid cascaded nonlinear compression approach

Youming Liu (刘又铭), Bowen Liu (刘博文), Youjian Song (宋有建)*, and Minglie Hu (胡明列)**

Ultrafast Laser Laboratory, Key Laboratory of Opto-electronic Information Science and Technology of Ministry of Education, School of Precision Instruments and Opto-electronics Engineering, Tianjin University, Tianjin 300072, China

*Corresponding author: yjsong@tju.edu.cn

**Corresponding author: huminglie@tju.edu.cn

Received July 23, 2022 | Accepted August 30, 2022 | Posted Online October 12, 2022

Ultrafast lasers with high repetition rate, high energy, and ultrashort pulse duration have enabled numerous applications in science and technology. One efficient route to generate such pulses is postcompression of high-power Yb-doped lasers. Here, we report on the generation of 24.5 fs pulses with an output energy of 1.6 μJ and a repetition rate of 500 kHz. The pulses are obtained by using a hybrid cascaded nonlinear compression of the pulses delivered by a Yb-based fiber chirped pulse amplification (CPA) system. In the first stage, the initial 390 fs laser pulses are compressed to 100.7 fs based on spectral broadening in three fused silica plates. In the second stage, the pulses have been shortened to sub-30 fs by means of nonlinear compression in a hollow-core fiber. Overall, we could achieve ~16 times temporal shortening with the proposed approach. The results show that our system can effectively generate few-cycle pulses at a relatively high repetition rate and high energy, which can benefit future possible applications.

Keywords: multiple-plate medium; hollow-core photonic crystal fiber; pulse compression.

DOI: 10.3788/COL202220.100006

1. Introduction

Sub-30 fs laser sources have attracted much attention due to their potential applications in the fields of attosecond pulse generation[1], extreme ultraviolet pulse generation[2], terahertz sensing[3], lightwave sculpting[4], nonlinear imaging[5], and femtosecond time-scale spectroscopy[6]. On the other hand, they are important platforms for exploring electron dynamics inside atoms, molecules, and solids[7–9] or in nanostructures[10]. Particularly, the increase in repetition rate could effectively increase the photon flux and the signal-to-noise ratio of such laser sources, which will further benefit the application. Therefore, there is a growing demand for high-energy, high repetition rate, sub-30 fs lasers. At present, laser systems that can directly generate high-energy few-cycle pulses are dominated by chirped-pulse-amplified mode-locked Ti:sapphire laser systems. Nevertheless, due to the limitation of factors such as the thermal effect of the laser crystal, the repetition rates of the Ti:sapphire laser systems are mostly a few kilohertz. Yb-based lasers could achieve a high repetition rate and high energy at the same time. To this end, the broadband Ti:sapphire lasers are gradually being replaced by Yb-based lasers. However, the pulse duration of the Yb lasers is at least a few hundred femtoseconds, determined by the emission bandwidth of the gain medium. In order to generate high-energy, high repetition rate pulses with sub-30 fs pulse duration or even few cycles, the nonlinear compression of Yb-based laser pulses has become a research hotspot.

In general, nonlinear pulse compression of a Yb fiber laser can be achieved in a variety of ways. Among all demonstrations, spectral broadening in bulk materials is the most concise and effective method to achieve nonlinear compression of pulses. When intense laser pulses are focused on a solid medium such as fused silica, it will cause a variety of nonlinear effects such as self-phase modulation (SPM), self-focusing, and self-steepening, thereby achieving pulse spectral broadening. However, in overly thick media, the strong self-focusing effect will induce the generation of ionization and filaments, which causes damage to the media[11]. Fortunately, in 2000, a paper presented the theory that self-phase modulated pulses with good beam quality can be obtained after repetitive passes through an extended nonlinear medium[12]. In 2014, the multiple-plate supercontinuum generation was experimentally demonstrated[13]. The researchers used multiple thin fused silica plates well positioned near the beam focus, balancing this destructive self-focusing through the divergence of the beam in the air. The technique of pulse compression by multiple-plate spectral broadening and phase compensation is called multiple-plate compression (MPC).

Since then, a number of research groups have made efforts to use MPC technology to obtain few-cycle pulses. For example, Lu *et al.* achieved the compression of 1030 nm laser pulses with pulse duration of 170 fs to 3.21 fs in a single cycle by a two-stage MPC system[14]; He *et al.* obtained a continuum covering 460 to 950 nm using seven thin solid plates and compressed the pulses to 5.4 fs[15]; Beetar *et al.* compressed 280 fs laser pulses to 18 fs using the MPC technique[16]; Tamming *et al.* obtained 3.3 fs pulses by a single MPC system and further used the pulses in a transient absorption spectroscopy experiment[17]. However, in order to meet the spectral broadening condition, which is high nonlinearity in bulk material, a high-energy pump laser source is required. At the energy of a few microjoules, it is difficult to obtain significant spectral broadening with this method.

In this regard, gas-filled hollow-core photonic crystal fibers (HC-PCFs) are another reliable pulse compression platform. In HC-PCFs, the beam is bound in the gas-filled fiber core due to the antiresonance effect of the cladding walls. The overlap between the propagation mode and the surrounding solid structures is very low, which avoids the problem of damage to solid materials and achieves high damage thresholds[18–20]. In addition, by adjusting the type of filling gas and the gas pressure, the HC-PCF can provide sufficient nonlinearity to support the spectral broadening of the pulses. Currently, great efforts have been made to invest pulse compression in HC-PCFs. Using a five-bar Xe-filled HC-PCF with a bore radius of 100 μm, Alencious *et al.* successfully achieved temporal compression from 320 to 61 fs[21]; Köttig *et al.* reported a two-stage system for compressing pulses from 320 to 3.8 fs with two HC-PCFs[22]; Schade *et al.* studied the scaling of soliton dynamics in noble gas-filled HC-PCFs and compressed 250 fs pulses at 1030 nm to ∼5 fs duration in an 80-cm-long HC-PCF[23].

In this work, we explore how to compress the pulses of a chirped pulse Yb-doped fiber amplifier with moderate pulse energy and intermediate repetition rate. In this paper, a hybrid cascading spectral broadening is realized by using MPC and HC-PCF. The initial pulse duration of 390 fs is compressed to 24.5 fs at a useful, intermediate repetition rate of 500 kHz, and the corresponding compression ratio is calculated to be ∼16. This technique may extend the prospects of realizing ultrashort pulse compression at moderate energy levels.

2. Experimental Setup

The experimental setup is shown in Fig. 1. The laser source is a commercial Yb-based laser system (BWT, BFL-1030-20L) with the output of 1030 nm, 12 μJ, 390 fs pulses at a repetition rate of 500 kHz. The right inset in Fig. 1 shows the autocorrelation trace of the pump source. A half-wave plate (HWP) is used to control the polarization of the pump beams to meet the high transmission orientation of the chirped mirrors. In the first stage, the laser pulses are focused to a beam waist of 0.25 mm with a 300 mm focal length lens (F1) to yield an intensity of 295 GW/cm^2. Three pieces of 2 mm thick fused silicon plates

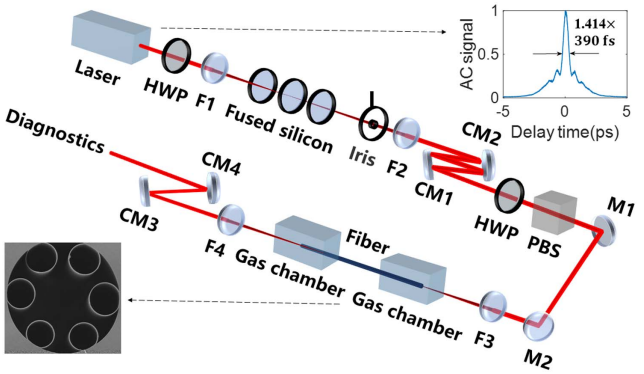

Fig. 1. Schematic of the experimental setup showing the two compression stages. F1–F4, lenses; M1, M2, reflective mirrors; CM1–CM4, chirped mirrors; HWP, half-wave plate; PBS, polarizing beam splitter. The right inset shows the autocorrelation trace of the laser source; the left inset in the setup represents the scanning electron micrograph of the HC-PCF with a core diameter of 68 μm and a wall thickness of ∼0.3 μm.

are placed near the focal point to broaden the spectrum. A spectrum analyzer (Yokogawa, AQ6315A) is used to characterize the spectrum. The position of the silica plates is determined empirically to be the position that results in the maximum spectral broadening and avoids optical damage or filament formation inside the fused silicon plate. To this end, the first fused silicon piece is placed before the focus, and the other two fused silicon plates are placed behind the focal point. The spacing between adjacent plates is measured to be 4.5 and 3 mm, respectively. Then, the beam is filtered with an iris aperture, leaving only the central part of the beam. As much as 8 μJ pulse energy is obtained, and the corresponding efficiency is calculated to be 67%. The remaining beam is collimated with a 100 mm focal length lens (F2). The spectrally broadened pulses are dechirped by a pair of chirped mirrors (Ultrafast Innovations, HD-65), which yield a total group delay dispersion (GDD) of −12,000 fs^2. We characterized and optimized the compressed pulses with an autocorrelator (APE GmbH, PulseCheck50).

In the second stage, we use an HWP and a polarizing beam splitter to control the pulse energy incident into the HC-PCF. The left inset of Fig. 1 represents the scanning electron micrograph of the HC-PCF with a core diameter of 68 μm and a wall thickness of ∼0.3 μm. The fiber is placed inside of the enclosed homemade gas chambers. Both chamber windows are sapphire plates, allowing the chambers to be filled with high-pressure gases without any damage. Using a lens (F3) with a focal length of 60 mm, the laser pulses are coupled into the fiber. In terms of coupling losses and Fresnel reflections at the uncoated windows of the gas chamber, a total transmission efficiency of about 53% is achieved for this 45-cm-long HC-PCF. In our experiment, the chambers are filled with high-purity argon gas to generate sufficient nonlinearity. With a focal length of 35 mm lens (F4), the beam is collimated, and the pulse duration of the output beam is further compressed by two chirped mirrors of the same type as those used in the first stage. Finally, the compressed laser pulses are diagnosed with the spectrum analyzer and autocorrelator.

3. Experimental Results and Analysis

In the first stage, nonlinear compression in the MPC is investigated. First, we consider the influence of different thicknesses of fused silica plates. In 3 mm fused silica plates, the spectrum is broadened to be wider. However, the conical emission becomes stronger due to the self-focusing effect, which causes the iris-filtered beam to retain only 30% of pump energy. In 1 mm thickness fused silica plates, the spectral broadening after passing through each fused silica plate is insignificant, and it is difficult to judge the appropriate position of the fused silicon plates by the spectrum displayed on the spectrum analyzer. To this end, we finally used 2 mm thick fused silicon plates in this stage. The spectra in a log scale are shown in Fig. 2(a). As can be seen, the spectrum of the pump gradually broadens by accumulating more plates. Finally, the generated spectrum covers from 1007 to 1053 nm at the −30 dB intensity level after passing through three plates. The spectral broadening in the three plates is basically symmetric to the pump spectrum, which indicates that the spectral broadening is determined by SPM. Thus, the resulting dispersion can be compensated for by the chirped mirrors mentioned above. The beam profile after the iris is shown in the inset of Fig. 2(a).

The compressed intensity autocorrelation trace is shown in Fig. 2(b), which has a full width at half-maximum (FWHM) duration of 153 fs. The intensity envelope and temporal phase of the pulse retrieved from the phase and intensity from correlation and spectrum only (PICASO) algorithm[24] are shown in Fig. 2(c), which reveals a 100.7 fs pulse. In addition, the transform-limited (TL) pulse for the first stage is calculated to be 91.6 fs, which is also plotted in Fig. 2(c). The reconstructed temporal pulse envelope is a little larger than that of the TL pulse, and possesses a residual tail. This is reasonable, considering the high-order dispersion of the pump laser pulses, which results in large pedestals of the pump pulses (as can be seen in the inset of Fig. 1). The high-order dispersion can be compensated by the chirped mirrors in the first stage.

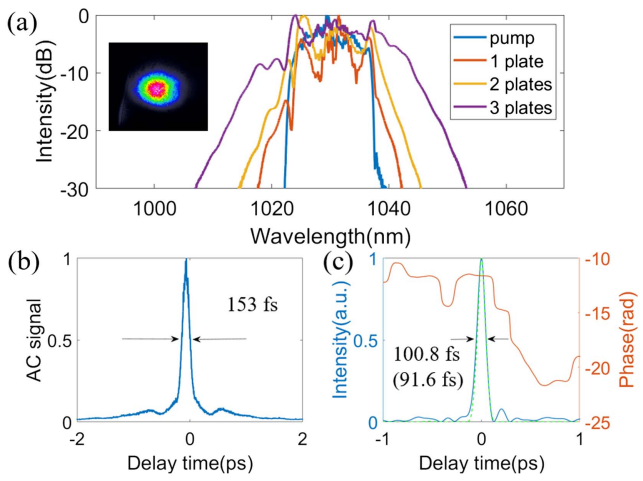

Fig. 2. Diagnosis results of the first stage. (a) Spectral broadening in log scale with different numbers of plates in the first stage; the inset is the beam profile after the iris. (b) Intensity autocorrelation trace after phase compensation in the first stage; (c) retrieved temporal intensity envelope and phase after phase compensation in the first stage by PICASO algorithm and the TL pulse.

In the second stage, we use an argon-filled HC-PCF for further pulse compression. The pump energy to this stage is controlled using a combination of HWP and polarizing beam splitter (PBS) cube. To avoid the accumulation of more nonlinear chirps that cannot be compensated for and to obtain a good pulse quality, the injection energy is adjusted to be 3 μJ. The HC-PCF used in our experiment is 45 cm long with core diameters of 68 μm. To understand the propagation dynamics within the HC-PCF, we first conduct a numerical model using the unidirectional pulse propagation equation (UPPE)[25,26]. Considering that the peak intensity of the pulses in the HC-PCF is about 207 GW/cm^2, only weak multiphoton ionization can occur[27], so the ionization term is neglected in the simulation. The dispersion of the fiber is approximated by the antiresonant tube model[28]. The group velocity dispersion (GVD) of an evacuated HC-PCF is anomalous at all wavelengths of the input pulses and can be compensated for by the normal dispersion of the filling gas. As the gas pressure increases, the zero-dispersion wavelength continues to redshift. At a gas pressure of 26 bar, the dispersion at the center wavelength is raised to 1 fs^2/cm and the zero-dispersion wavelength point is moved to 1116 nm, which makes the whole spectral range of the output pulses of the first stage lie in the normal dispersion region. The dispersion curve of the HC-PCF is shown in Fig. 3(b). To be more precise, the experimental results of the first stage are used as input data in the simulation. Figure 3(a) shows the nonlinear pulse dynamics in the fiber. As can be seen, strong spectral broadening is observed. The output spectrum in a log scale is shown in Fig. 3(b). The modulations in the central part of the spectrum can be associated with spectral features of the input spectrum. The experimental results are also presented in Fig. 3(b), which match the simulation well. The difference between the simulation and experiment is mainly due to the fact that the dispersion model cannot perfectly match the actual dispersion of the fiber. The broadened spectrum in our experiment covers from 900 to 1120 nm at the −30 dB intensity level. In the process of spectral broadening, SPM plays a major role. Additionally, self-steepening also affects spectral broadening, which makes a stronger spectral extension to shorter wavelengths. Almost the entire spectral range of the pulse output from the fiber lies in the normal dispersion region. To this end, we use a pair of

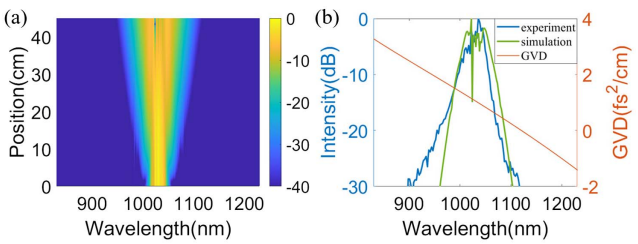

Fig. 3. (a) Simulated spectral evolutions in the 45-cm-long HC-PCF; (b) experimental and simulated spectral outputs are compared. The red line indicates the GVD.

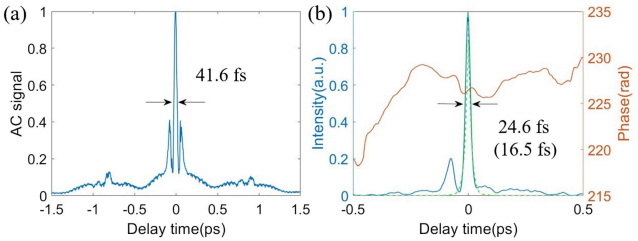

Fig. 4. (a) Intensity autocorrelation trace of the 1.6 μJ pulses after phase compensation in the second stage; (b) retrieved temporal intensity envelope and phase of the 1.6 μJ pulses after phase compensation in the second stage by PICASO algorithm and the TL pulse.

negatively chirped mirrors to compensate for the chirp. The dispersion provided by the two chirped mirrors not only compensates for the positive chirp introduced by spectral broadening, but also by all the optical elements after the fiber, which enables the detection of sub-30 fs pulse duration.

Figure 4(a) shows the autocorrelator measurement of the pulses after the second compression stage, which has an intensity FWHM of 41.6 fs. Figure 4(b) shows the corresponding temporal shape and phase of the output pulse retrieved by the PICASO algorithm, with a pulse duration of 24.6 fs. The 16.5 fs TL pulse calculated from the experimentally measured spectrum is also shown in Fig. 4(b). Both the autocorrelation trace and the retrieved pulse have pedestals, which are mainly caused by the residual higher-order dispersion that cannot be compensated for by the chirped mirrors. At higher output pulse energies, the pedestal of the compressed pulse will be larger. We increased the output pulse energy to 2 μJ; the autocorrelation trace obtained after compression is shown in Fig. 5. The pedestal becomes so large that the pulse duration of the main peak becomes hard to read out. The nonlinear chirp which is difficult to compensate for partly originates from the initial pulse, and the other part originates from the complex nonlinear effects in the HC-PCF. As the energy of the input pulses increases, the nonlinear effects in the HC-PCF increase, which also leads to the increase of the nonlinear chirp accumulated in the HC-PCF, forming a larger pedestal. To this end, injection pulse energy of the second stage is controlled, and the output pulse

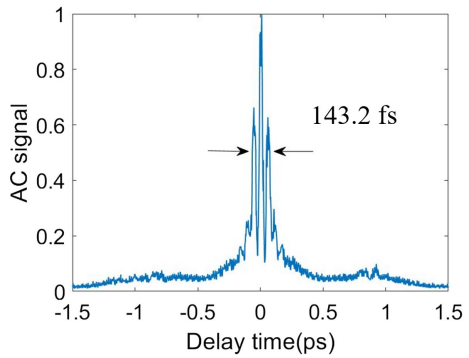

Fig. 5. Intensity autocorrelation trace of the 2 μJ pulses after phase compensation in the second stage.

energy is measured to be 1.6 μJ. However, it is possible to further expand the broadened pulse spectrum and obtain shorter pulse duration at the output of the HC-PCF by adopting well-designed chirped mirrors.

4. Conclusions

In summary, we demonstrated an efficient hybrid cascaded compression system combining an MPC and HC-PCF setup. Pulse shortening from 390 fs duration to less than 30 fs at 500 kHz repetition rate and 1.6 μJ of pulse energy has been realized. In our system, the output power of initial laser source is limited to be 12 μJ. Neither a single MPC stage nor an HC-PCF stage is sufficient to compress the pulse down to sub-30 fs pulse duration. A two-stage HC-PCF method could solve this problem by sacrificing the simplicity and compactness of the system. For the goal of producing sub-30 fs pulses, we find our solution, a hybrid cascaded system, is a very good compromise, since the first stage does not need complex optical path alignment. Given more suitable dispersion compensation devices, shorter pulses down to few cycles or even single cycle could be expected. Our system demonstrates the potential of the proposed hybrid compression stage to efficiently generate broad supercontinuum and few-cycle pulses from a high repetition rate and moderate pulse energy Yb-based laser source.

Acknowledgement

This work was supported by the National Natural Science Foundation of China (NSFC) (Nos. 62105237, 61827821, and 61975144).

References

1. F. Krausz and M. Ivanov, "Attosecond physics," Rev. Mod. Phys. **81**, 163 (2009).
2. Y. Jia, L. Guo, S. Hu, X. Jia, D. Fan, R. Lu, S. Han, and J. Chen, "Time-energy analysis of the photoionization process in a double-XUV pulse combined with a few-cycle IR field," Chin. Opt. Lett. **19**, 123201 (2021).
3. N. Horiuchi, "Endless applications," Nat. Photonics **4**, 140 (2010).
4. E. Goulielmakis, V. S. Yakovlev, A. L. Cavalieri, M. Uiberacker, V. Pervak, A. Apolonski, R. Kienberger, U. Kleineberg, and F. Krausz, "Attosecond control and measurement: lightwave electronics," Science **317**, 769 (2007).
5. D. Polli, V. Kumar, C. M. Valensise, M. Marangoni, and G. Cerullo, "Broadband coherent Raman scattering microscopy," Laser Photonics Rev. **12**, 1800020 (2018).
6. M. Maiuri, M. Garavelli, and G. Cerullo, "Ultrafast spectroscopy: state of the art and open challenges," J. Am. Chem. Soc. **142**, 3 (2020).
7. L. Young, K. Ueda, M. Gühr, P. H. Bucksbaum, M. Simon, S. Mukamel, N. Rohringer, K. C. Prince, C. Masciovecchio, M. Meyer, A. Rudenko, D. Rolles, C. Bostedt, M. Fuchs, D. A. Reis, R. Santra, H. Kapteyn, M. Murnane, H. Ibrahim, F. Légaré, M. Vrakking, M. Isinger, D. Kroon, M. Gisselbrecht, A. L'Huillier, H. J. Wörner, and S. R. Leone, "Roadmap of ultrafast X-ray atomic and molecular physics," J. Phys. B **51**, 032003 (2018).
8. S. R. Leone, C. W. McCurdy, J. Burgdoerfer, L. S. Cederbaum, Z. Chang, N. Dudovich, J. Feist, C. H. Greene, M. Ivanov, R. Kienberger, U. Keller, M. F. Kling, Z. H. Loh, T. Pfeifer, A. N. Pfeiffer, R. Santra, K. Schafer, A. Stolow, U. Thumm, and M. J. J. Vrakking, "What will it take to observe processes in 'real time?'" Nat. Photonics **8**, 162 (2014).

9. M. Nisoli, P. Decleva, F. Calegari, A. Palacios, and F. Martín, "Attosecond electron dynamics in molecules," Chem. Rev. **117**, 10760 (2017).
10. P. Dombi, Z. Pápa, J. Vogelsang, S. V. Yalunin, M. Sivis, G. Herink, S. Schäfer, P. Groß, C. Ropers, and C. Lienau, "Strong-field nano-optics," Rev. Mod. Phys. **92**, 025003 (2020).
11. M. Seidel, G. Arisholm, J. Brons, V. Pervak, and O. Pronin, "All solid-state spectral broadening: an average and peak power scalable method for compression of ultrashort pulses," Opt. Express **24**, 9412 (2016).
12. N. Milosevic, G. Tempea, and T. Brabec, "Optical pulse compression: bulk media versus hollow waveguides," Opt. Lett. **25**, 672 (2000).
13. C. H. Lu, Y. J. Tsou, H. Y. Chen, B. H. Chen, Y. C. Cheng, S. D. Yang, M. C. Chen, C. C. Hsu, and A. H. Kung, "Generation of intense supercontinuum in condensed media," Optica **1**, 400 (2014).
14. C. H. Lu, W. H. Wu, S. H. Kuo, J. Y. Guo, M. C. Chen, S. D. Yang, and A. H. Kung, "Greater than 50 times compression of 1030 nm Yb:KGW laser pulses to single-cycle duration," Opt. Express **27**, 15638 (2019).
15. P. He, Y. Liu, K. Zhao, H. Teng, X. He, P. Huang, H. Huang, S. Zhong, Y. Jiang, S. Fang, X. Hou, and Z. Wei, "High-efficiency supercontinuum generation in solid thin plates at 0.1 TW level," Opt. Lett. **42**, 474 (2017).
16. J. E. Beetar, S. Gholam-Mirzaei, and M. Chini, "Spectral broadening and pulse compression of a 400 μJ, 20 W Yb:KGW laser using a multi-plate medium," Appl. Phys. Lett. **112**, 051102 (2018).
17. R. R. Tamming, C. Y. Lin, J. M. Hodgkiss, S. D. Yang, K. Chen, and C.-H. Lu, "Single 3.3 fs multiple plate compression light source in ultrafast transient absorption spectroscopy," Sci. Rep. **11**, 12847 (2021).
18. B. Beaudou, F. Gerôme, Y. Y. Wang, M. Alharbi, T. D. Bradley, G. Humbert, J. L. Auguste, J. M. Blondy, and F. Benabid, "Millijoule laser pulse delivery for spark ignition through kagome hollow-core fiber," Opt. Lett. **37**, 1430 (2012).
19. O. H. Heckl, C. R. E. Baer, C. Kränkel, S. V. Marchese, F. Schapper, M. Holler, T. Südmeyer, J. S. Robinson, J. W. G. Tisch, F. Couny, P. Light, F. Benabid, and U. Keller, "High harmonic generation in a gas-filled hollow-core photonic crystal fiber," Appl. Phys. B **97**, 369 (2009).
20. Y. Y. Wang, X. Peng, M. Alharbi, C. F. Dutin, T. D. Bradley, F. Gérôme, M. Mielke, T. Booth, and F. Benabid, "Design and fabrication of hollow-core photonic crystal fibers for high-power ultrashort pulse transportation and pulse compression," Opt. Lett. **37**, 3111 (2012).
21. S. Z. A. Lo, L. Wang, and Z. H. Loh, "Pulse propagation in hollow-core fiber at high-pressure regime: application to compression of tens of μJ pulses and determination of nonlinear refractive index of xenon at 1.03 μm," Appl. Opt. **57**, 4659 (2018).
22. F. Köttig, D. Schade, J. R. Koehler, P. St.J. Russell, and F. Tani, "Efficient single-cycle pulse compression of an ytterbium fiber laser at 10 MHz repetition rate," Opt. Express **28**, 9099 (2020).
23. D. Schade, F. Köttig, J. R. Koehler, M. H. Frosz, P. S. J. Russell, and F. Tani, "Scaling rules for high quality soliton self-compression in hollow-core fibers," Opt. Express **29**, 19147 (2021).
24. J. W. Nicholson, J. Jasapara, W. Rudolph, F. G. Omenetto, and A. J. Taylor, "Full-field characterization of femtosecond pulses by spectrum and cross-correlation measurements," Opt. Lett. **24**, 1774 (1999).
25. F. Meng, B. Liu, S. Wang, J. Liu, Y. Li, C. Wang, A. M. Zheltikov, and M. Hu, "Controllable two-color dispersive wave generation in argon-filled hypocycloid-core kagome fiber," Opt. Express **25**, 32972 (2017).
26. W. Chang, A. Nazarkin, J. C. Travers, J. Nold, P. Hölzer, N. Y. Joly, and P. St.J. Russell, "Influence of ionization on ultrafast gas-based nonlinear fiber optics," Opt. Express **19**, 21018 (2011).
27. A. Couairon and A. Mysyrowicz, "Femtosecond filamentation in transparent media," Phys. Rep. **441**, 47 (2007).
28. M. Zeisberger and M. A. Schmidt, "Analytic model for the complex effective index of the leaky modes of tube-type anti-resonant hollow core fibers," Sci. Rep. **7**, 11761 (2017).